IOSR Journal of Applied Physics (IOSR-JAP)
e-ISSN: 2278-4861.Volume 7, Issue 3 Ver. III (May. - Jun. 2015), PP 56-62
www.iosrjournals.org

Maps of S-Z effect on Clusters of Galaxies

Enkelejd Çaça
Physic Department Faculty of Mathematics Engineering and Physics Engineering Polytechnic University of Tirana Tirana, Mother Theresa Square Nr.5

Abstract: *We present an analysis of 16 clusters of galaxies, focusing on the comptonization structure of the intracluster medium. The main goal is to provide accurate maps of the S-Z effect in order to select those clusters whom offer the possibility of creating images when observed with multipixel systems. We used data from X-ray observations to simulate the S-Z effect. For at least 4 rich and extended clusters the maps show that we can form a moderate image. For the other clusters only the central bin is observable and distinguishable from the primary anisotropy of the Cosmic Microwave Background (CMB).*
Keywords**:** *Cluster of Galaxies, X-ray, Comptonization, Cooling Flow, S-Z effect*

I. Introduction

Over the last four decades, much effort has been put in trying to achieve the observational goal of detecting and imaging the Synyaev-Zel'dovich (SZ) effect from cluster of galaxies, first proposed in 1970-s [1], [2] as a consequence of Compton interaction between Cosmic Microwave Background (CMB) photons and highly energetic electrons present in the hot plasma of intergalactic space within cluster of galaxies (intra-cluster medium, ICM). The effect resulting in a CMB anisotropy with characteristic spectral signature and spatial correlation with cluster position in the sky, and most of of all its nearly complete independence from the cluster redshift, was soon designated as one of the most reliable and rich source of information for both cluster physics and cosmology, due to its simplest physical interpretation and marginal detection possibilities even with the observation techniques and detector technology of 20 years ago. While imaging of the SZ effect has already been performed at radio frequencies [3], [4] with the aid of interferometric detectors, higher frequency measurements have been mostly performed from single-pixel detectors, with the only (but significant) advantage of multi-band selection and higher spectral discrimination of the signal from unwanted contributions. Now, finally, the advance in bolometer technology and the know-how of the past decades suggest that present and the near-future microwave instruments pretending to extract the largest astrophysical and cosmological information from SZ observation must be able to combine multi-frequency techniques with moderate-to-high imaging capabilities. In order to significantly reduce the bulk of systematic and statistical uncertainty coming from the modeling of ICM density and temperature distributions and, for ground-based experiment, take full advantage of long integration and on-site operator control to optimally customize the observation strategy. From e purely instrumental point of view, it appeared that, even with the largest advantage of high flux collection efficiency of the wide field single pixel configuration, the averaging of atmospheric fluctuations over large scale brought significant contribution to the sky noise detected with the 3-field modulation strategy. Moreover, giving the growing sky coverage capabilities of the new experiments like MAD (Multi Array of Detector) it will soon be possible to perform routine observations and produce un target surveys of potentially more than 100 clusters, to determine statistically robust cosmological parameter estimates and deeply probe the universe at high red-shift.
This paper is organised as follows: in §2. we provide temperature and density profile. In §3. The comptonization parameters y_0 are presented, in §4. we provide the conclusions.

II. Temperature And Density Profiles.

In order to simulate the spatial distribution of the comptonization parameter we need to build the temperature and density profile using data from X-ray observations. So far we use the isothermal model for the temperature profile, assuming a spherical symmetry of the ICM. This assumption is not e god approximation for the real distribution of the gas. Observations on X-ray band suggest that in some clusters we have a flow of the gas at the center of cluster (Cooling Flow CF), where the cooling time is much lower than that of the rest of the gas, typically the cooling time scale it's $\sim 10^7$Gy much lower than a typically cooling time of $\sim 10^{10}$Gy.

Table 1. Cluster sample.

Cluster	Right ascension *J2000.0*	Declination *J2000.0*	*z*	
MS 0451.6	04h54m10.9s	-3.0186 0.550000 (3) NO	0.550000 (3)	NO-CF
MS 1054.4	0321h57m00.3s	-3.62472	0.829700 (3)	NO-CF
ABELL 773	09h17m59s	51.7064	0.217000 (1)	CF
MS 1358.4+6245	13h59m54.3s	62.5101	0.328000 (2)	CF
RXJ 1347				CF
ZW 3146	10h23m39.63s	4.18621	0.290600 (3)	CF
ABELL 1795	13h49m00s	26.5852	0.062476	CF
ABELL 2261 17h22m28s	17h22m28s	32.1535	0.224000 (1)	NO-CF
ABELL 2218	16h34m54s	66.2167	0.175600(1)	NO-CF
ABELL 1689	13h11m34s	-1.3654	0.183200(1)	NO-CF
ABELL 1413	11h55m18.9s	23.40861	0.142700(1)	NO-CF
ABELL 697	08h42m53s	36.3365	0.282000(1)	NO-CF
ABELL 1835	14h01m02s	2.8588	0.253200 (1)	CF
ABELL 2204	16h32m45s	5.5785	0.152158 (1)	CF
ABELL 2390	21h53m34s	17.6697	0.228000 (1)	CF

(1) Right ascension, Declination and z reference [5].
(2) Right ascension, Declination and z reference [6].
(3) Right ascension, Declination and z reference [7], [8]

Temperature and density profiles are discussed in more details in a previous paper [9], however we remember shortly the X-ray analysis that we use. In the case of the CF clusters in order to modelling the gas temperature we use a non-isothermal model for the temperature [10], [11], [12]. The temperature declines from the maximum cluster temperature at a break radius r_{br} moving outwards and shows the characteristic temperature decline towards the X-ray emission peak. Hence, for each cluster we select temperature bins inside the radius $R_{T,max} = r_{br}$ and fit them using the following expressions:

$$T_r = T_0 + T_1 \frac{(r/r_T)^{\mu}}{1+(r/r_T)^{\mu}} \quad (1)$$

$$\tilde{T}_r = \tilde{T}_0 - \tilde{T}_1 \exp(-\frac{r^2}{2\tilde{r}_T^2}) \quad (2)$$

In order to reduce the number of parameters here, we set T(r = 0) equal to the temperature of the central bin for both fits and use μ=2 in Eq.1 [13].

Another parameter to be defined is the electronic density of the gas and its profile. We model the gas density by using a single β-model given by:

$$n_r = n_0 \left(1 + \left(\frac{r}{r_c}\right)^2\right)^{-\frac{3\beta}{2}} \quad (3)$$

An alternative parametrization of the gas density profile is the more complex double β-model [14], which is a popular generalization of the single β-model [15], [16] used to model the central surface brightness excess observed in CF clusters.

$$n_r = n_1 \left(1 + \left(\frac{r}{r_{c1}}\right)^2\right)^{-\frac{3\beta 1}{2}} + n_2 \left(1 + \left(\frac{r}{r_{c2}}\right)^2\right)^{-\frac{3\beta 2}{2}} \quad (4)$$

III. Comptonization Parameter Y

To calculate the Comptonization parameter, we use the temperature and density profiles obtained above integrating over the line of sight (l.o.s) through the cluster yields the non-relativistic (*i.e* low electron temperature) expression for the spectrum of the thermal SZ effect [17], [18]:

$$\Delta I_t = i_0 y g(x) \quad (5)$$

where $i_0 = 2(kT_{CMB})^3/(hc)^2$, and y is the *comptonization* parameter defined as:

$$y = \int_{l.o.s} n_e\,(l) \frac{kT_e}{m_e c^2} \sigma_T dl = \frac{kT_e}{m_e c^2} \tau \quad (6)$$

i.e. an integral of electron density and temperature profiles across the cluster; σ_T is the Thomson cross section, and τ is the cluster optical depth with respect to the Thomson scattering proces. The dependence from the non dimensional frequency, is entirely described by;

$$g(x) = \frac{x^4 e^x}{(e^x-1)}\left[x\frac{e^x+1}{e^x-1} - 1\right] \tag{7}$$

Eq. 7 shows that the distortion is negative at low frequencies below the critical *crossover* value $x_0 \approx 3.83$ (corresponding to $\sim 217GHz$) and positive in the high frequency region. The Comptonization parameters that we use to build the maps are shown in Table. 2

Table 2. In this table we show the comptonization parameter for the clusters in question. For the cluster with cooling flow (CF) has been obtained applying the temperature profile see Eqs. 1 and 2.

Cluster	y_0 (CF)	y_0 (Isothermal)	y_0 ($T_e profile$)	
ABELL 697	–	$1.4x10^{-4}$	–	NO-CF
ABELL 773	$4.5x10^{-4}$	$7.06x10^{-4}$	–	CF
MS 0451.6	–	$2.99x10^{-4}$	$2.85x10^{-4}$	NO-CF
MS1054.4	–	$1.42x10^{-4}$	$1.40x10^{-4}$	NO-CF
MS 1358.4	$7.88x10^{-4}$	$12.8x10^{-4}$	–	CF
RXJ 1347	$9.18x10^{-4}$	$9.52x10^{-4}$	–	CF
ZW 3146	$6.2x10^{-4}$	$9.1x10^{-4}$	–	CF
ABELL 1413		$1.3x10^{-3}$	$1.17x10^{-3}$	NO-CF
ABELL 1795	8.02^{-6}	$1.5x10^{-5}$	–	CF
ABELL 1835	$6.28x10^{-4}$	$1.31x10^{-3}$	–	CF
ABELL 2163	$2.8x10^{-4}$	$3.26x10^{-4}$		CF
ABELL 1689		$4.64x10^{-4}$	$4.51x10^{-4}$	CF
ABELL 2204	$5.3x10^{-4}$	$8.11x10^{-4}$		CF
ABELL 2218		$3.38x10^{-3}$	$2.6x10^{-3}$	NO-CF
ABELL 2261		$4.79x10^{-4}$	$4.71x10^{-4}$	NO-CF
ABELL 2390	$3.99x10^{-4}$	$6.18x10^{-4}$	–	CF

In order to have a complete picture of S-Z thermal distortion we use X-ray data to calculate the comptonization parameter for the temperature and density parameters, for the computation of the cluster optical depth, and to map the amplitude of the effect in regions that are far away from the cluster center. The most commonly used approach is that found in [15] the so-called isothermal β-model for the Non Cooling Flow clusters, and the CF profile for the Cooling Flow clusters. The projected electron number density in the sky turns out to be:

$$n_e(r) = n_{e0}\left(1 + \frac{r^2}{r_c^2}\right)^{-\frac{3}{2}\beta} \tag{8}$$

Where r_c is the core radius representing the characteristic length scale of this model, and, the typicall values for β are 0.5-08, the corresponding τ and y profiles become

$$\tau_e(\theta) = \tau_{e0}\left(1 + \frac{\theta^2}{\theta_c^2}\right)^{\frac{1}{2}-\frac{3}{2}\beta} \tag{9}$$

$$y_e(\theta) = y_0\left(1 + \frac{\theta^2}{\theta_c^2}\right)^{\frac{1}{2}-\frac{3}{2}\beta} \tag{10}$$

where the central values are:

$$\tau_e(\theta) = \tau_{e0}\sigma_T\sqrt{\pi}\frac{\Gamma\left(\frac{3}{2}\beta-\frac{1}{2}\right)}{\Gamma\left(\frac{3}{2}\beta\right)} \tag{11}$$

$$y_0 = \tau_{e0}\frac{kT_e}{m_e c^2} \tag{12}$$

Where Γ, is the gama funciton.. Typical values of the *y* parameter are $\sim 10^{-4}$ in rich and/or moderately hot clusters. In the above calculation of the comptonization parameter, the angular separation from the cluster center has been inserted by means of well known transformation $r \approx \theta D_A$ which makes use of the angular diameter distance D_A.

All the clusters have been set at the same Angular Distance (~ 20 arcmin), comparable with the total field of bolometer array (~17arcmin), to a resolution of 4.5'/pixel. We use in this simulation the temperature profile of the Eq. 1 and Eq. 2 for all the cluster that show a CF center.
The resulting maps of this analysis are shown in Fig. 1, Fig. 2 and Fig. 3.

Figure.1

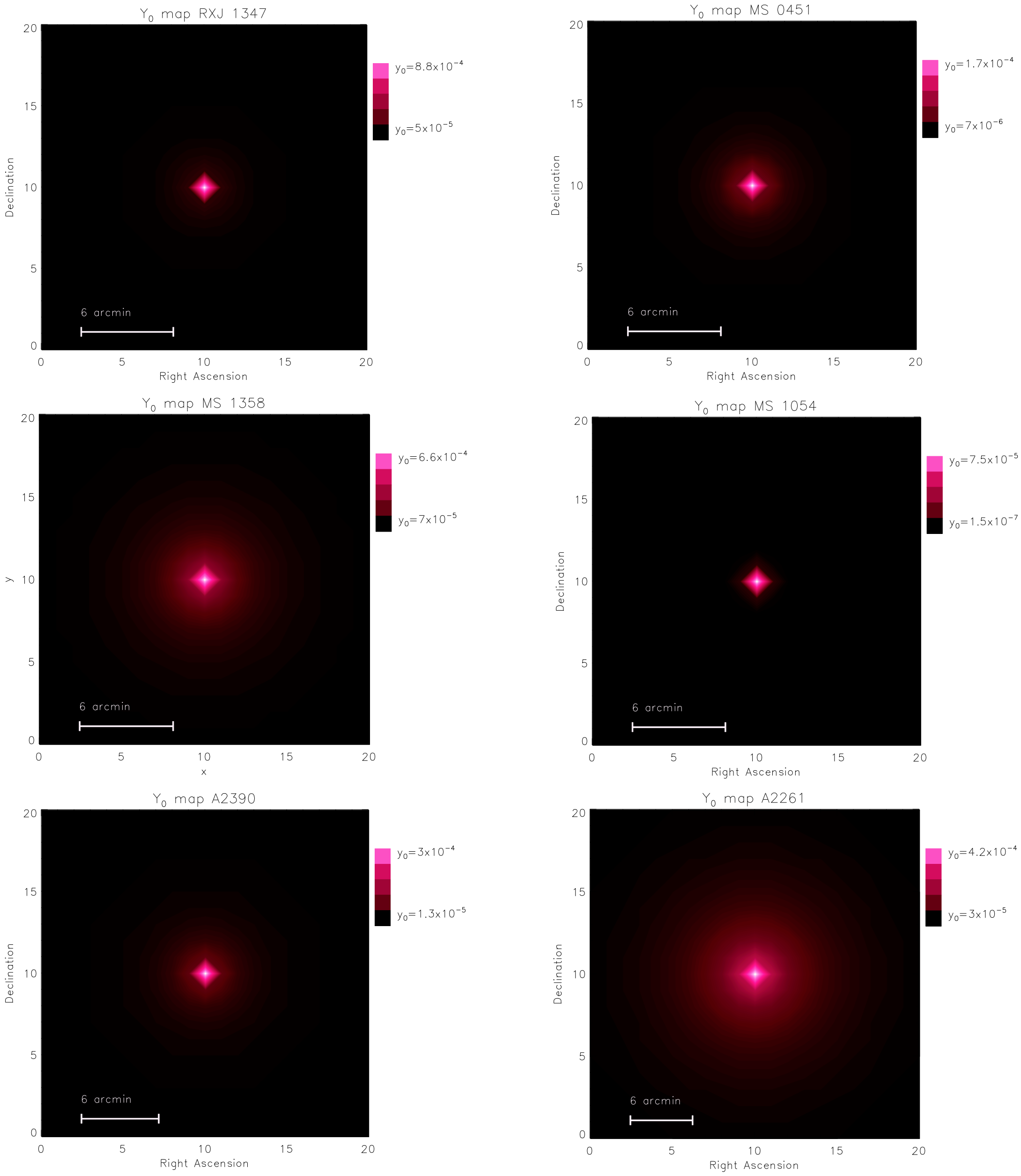

Figure 2.

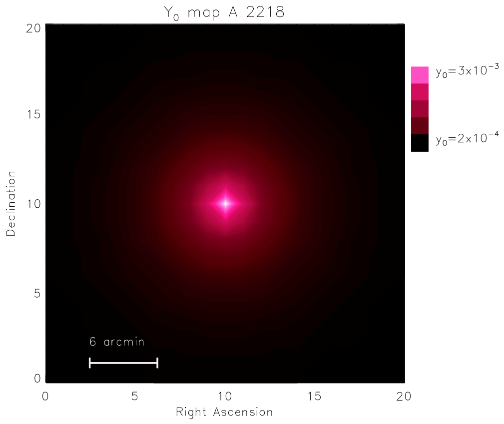
Y_0 map A 2218
$y_0=3\times10^{-3}$
$y_0=2\times10^{-4}$
6 arcmin
Declination
Right Ascension

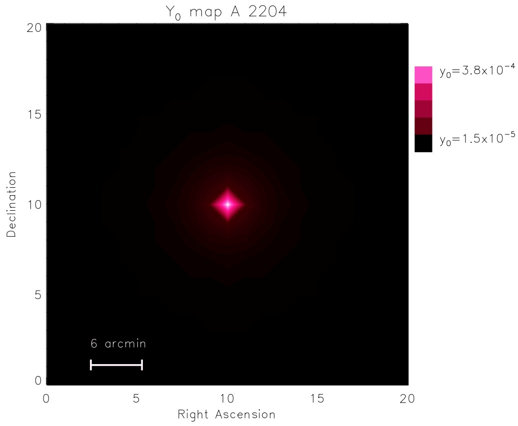
Y_0 map A 2204
$y_0=3.8\times10^{-4}$
$y_0=1.5\times10^{-5}$
6 arcmin
Declination
Right Ascension

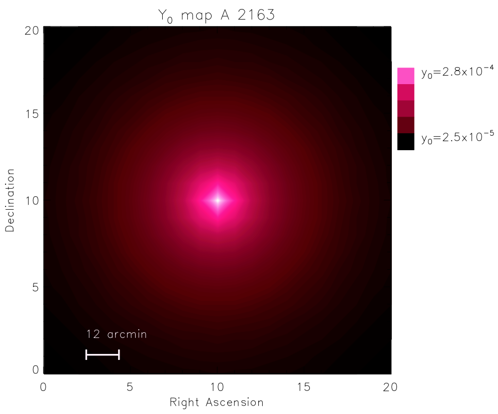
Y_0 map A 2163
$y_0=2.8\times10^{-4}$
$y_0=2.5\times10^{-5}$
12 arcmin
Declination
Right Ascension

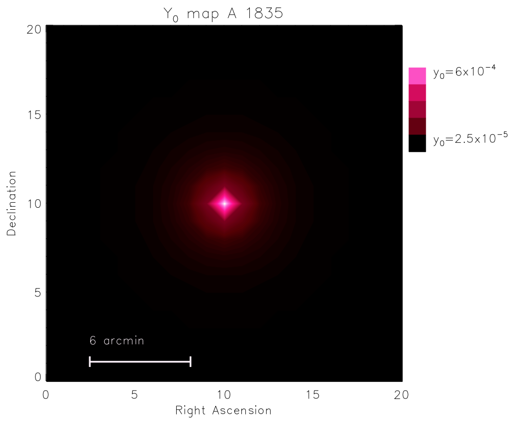
Y_0 map A 1835
$y_0=6\times10^{-4}$
$y_0=2.5\times10^{-5}$
6 arcmin
Declination
Right Ascension

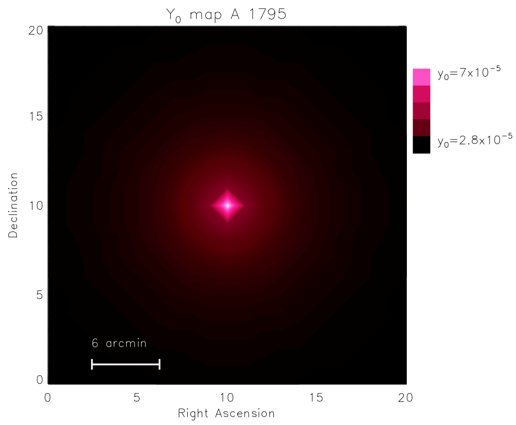
Y_0 map A 1795
$y_0=7\times10^{-5}$
$y_0=2.8\times10^{-5}$
6 arcmin
Declination
Right Ascension

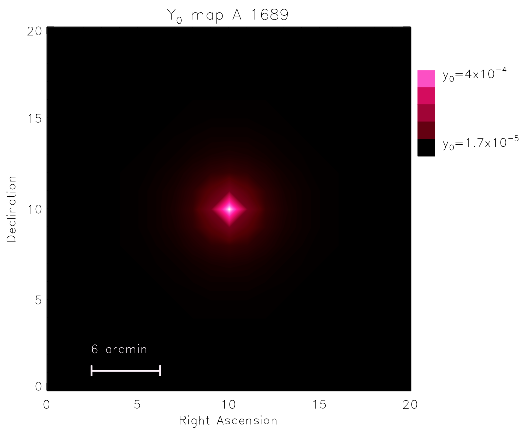
Y_0 map A 1689
$y_0=4\times10^{-4}$
$y_0=1.7\times10^{-5}$
6 arcmin
Declination
Right Ascension

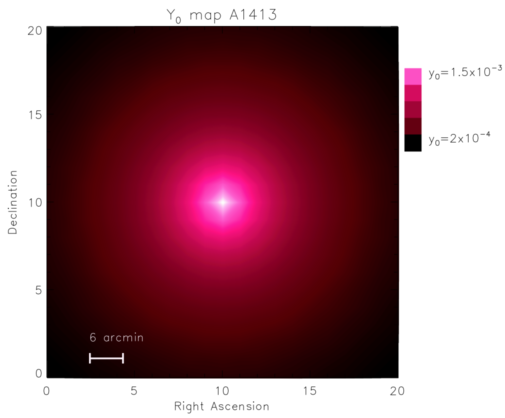
Y_0 map A1413
$y_0=1.5\times10^{-3}$
$y_0=2\times10^{-4}$
6 arcmin
Declination
Right Ascension

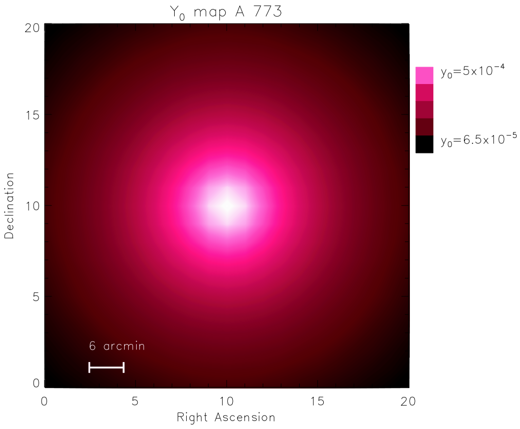
Y_0 map A 773
$y_0=5\times10^{-4}$
$y_0=6.5\times10^{-5}$
6 arcmin
Declination
Right Ascension

Figure 3.

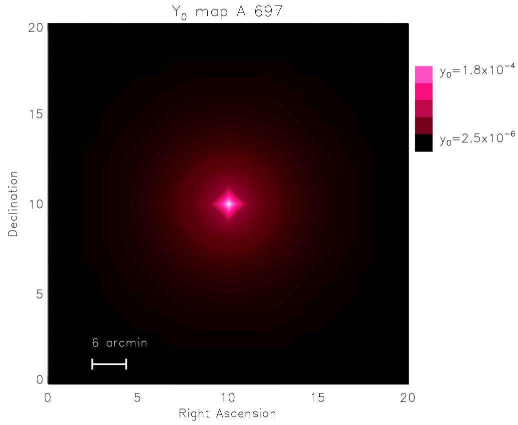
Y_0 map A 697
$y_0=1.8\times10^{-4}$
$y_0=2.5\times10^{-6}$
6 arcmin
Declination
Right Ascension

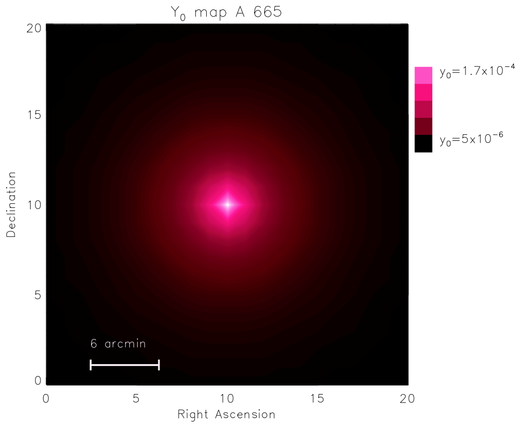
Y_0 map A 665
$y_0=1.7\times10^{-4}$
$y_0=5\times10^{-6}$
6 arcmin
Declination
Right Ascension

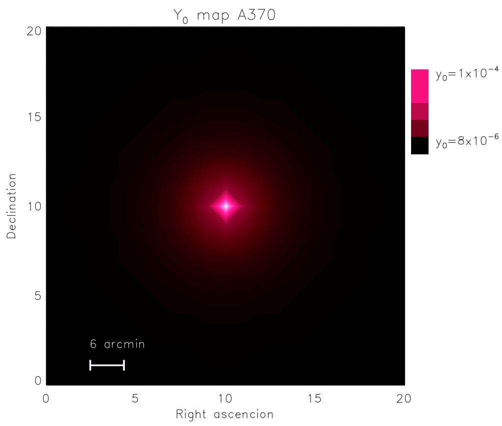
Y_0 map A370
$y_0=1\times10^{-4}$
$y_0=8\times10^{-6}$
6 arcmin
Declination
Right ascencion

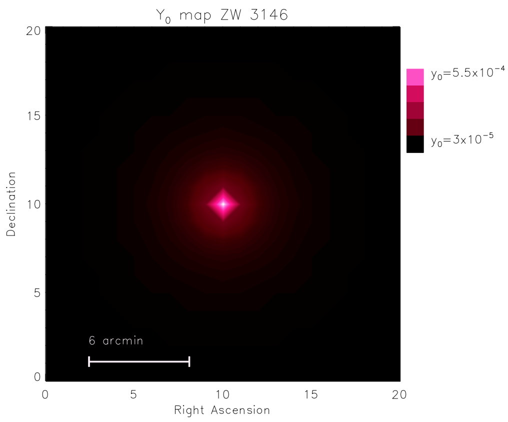
Y_0 map ZW 3146
$y_0=5.5\times10^{-4}$
$y_0=3\times10^{-5}$
6 arcmin
Declination
Right Ascension

IV. Conclusion

In this paper we simulate the spatial distributions of the comptonization parameter building maps of the change in the CMB spectrum from the S-Z effect. The sample in question includes a large number of 16 clusters. The main goal is to provide the possible clusters that can be target for multi-pixel observations, from which we can create a moderate image from multi-pixel observations on the infrared region of spectrum. The simulations using X-ray data show that for a number of nearby and rich clusters the comptonization of CMB radiation is well measurable and at the order of 10-4 even far away from the center of the clusters. For two clusters A2218 and A1413 the central value is 10 times greater than that of a normal cluster. So, the possibility of imaging the change and a morphological study of those clusters is quite possible. For other 3 clusters A2261, A2163 and A773 the effect is distributed quite well on the 20 arcmin field of view, except for the far outer regions, where it becomes comparable with the primary anisotropy of the CMB. However even for these clusters we have the possibility for an moderate capability imaging. For the other clusters the only the central bean show a measurable affect and so, becoming too weak to have a spatial division between pixels.

References

[1] R. A. Sunyaev and Y. B. Zeldovich. Distortions of the Background Radiation Spectrum. Nature , 223:721–722, August 1969. doi: 10.1038/223721a0.

[2] R. A. Sunyaev and Y. B. Zeldovich. The Observations of Relic Radiation as a Test of the Nature of X-Ray Radiation from the Clusters of Galaxies. *Comments on Astrophysics and Space Physics*, 4:173, November 1972.

[3] J. E. Carlstrom, M. Joy, and L. Grego. Interferometric Imaging of the Sunyaev-Zeldovich Effect at 30 GHz. ApJL, 456:L75, January 1996. doi: 10.1086/309866.

[4] L. Grego, J. Carlstrom, M. Joy, and W. Holzapfel. The Sunyaev–Zel'dovich Effect Imaged in Galaxy Clusters. In *American Astronomical Society Meeting Abstracts*, volume 28 of *Bulletin of the American Astronomical Society*, page 115.05, December 1996.

[5] M. F. Struble and H. J. Rood. A Compilation of Redshifts and Velocity Dispersions for ACO Clusters. ApJS, 125: 35–71, November 1999. doi: 10.1086/313274.

[6] J. T. Stocke, S. L. Morris, I. M. Gioia, T. Maccacaro, R. Schild, A. Wolter, T. A. Fleming, and J. P. Henry. The Einstein Observatory Extended Medium-Sensitivity Survey. II - The optical identifications. ApJS, 76:813–874, July 1991. doi: 10.1086/191582.

[7] G. A. Luppino and I. M. Gioia. Constraints on cold dark matter theories from observations of massive x-ray- luminous clusters of galaxies at high redshift. ApJL, 445:L77–L80, June 1995. doi: 10.1086/187894.

[8] I. M. Gioia and G. A. Luppino. The EMSS catalog of X-ray-selected clusters of galaxies. 1: an atlas of CCD images of 41 distant clusters. ApJS, 94:583–614, October 1994. doi: 10.1086/192083.

[9] Çaça. E. Change on the S-Z effect induced by the Cooling Flow (CF) on the hot electronic gas at the center of the clusters of galaxies. *Submitted for publictions*.

[10] R. Piffaretti, P. Jetzer, J. S. Kaastra, and T. Tamura. Temperature and entropy profiles of nearby cooling flow clusters observed with XMM-Newton. AAP, 433:101–111, April 2005. doi: 10.1051/0004-6361:20041888.

[11] R. Piffaretti and J. S. Kaastra. Effervescent heating: constraints from nearby cooling flow clusters observed with XMM-Newton. AAP, 453:423–431, July 2006. doi: 10.1051/0004-6361:20054365.

[12] M. Gitti, R. Piffaretti, and S. Schindler. Mass distribution in the most X-ray-luminous galaxy cluster RX J1347.5-1145 studied with XMM-Newton. AAP, 475:441–441, November 2007. doi: 10.1051/0004- 6361:20077580e.

[13] S. W. Allen, R. W. Schmidt, and A. C. Fabian. The X-ray virial relations for relaxed lensing clusters observed with Chandra. , 328:L37–L41, December 2001. doi: 10.1046/j.1365-8711.2001.05079.x.

[14] J. J. Mohr, B. Mathiesen, and A. E. Evrard. Properties of the Intracluster Medium in an Ensemble of Nearby Galaxy Clusters. A&A, 517:627–649, June 1999. doi: 10.1086/307227.

[15] A. Cavaliere and R. Fusco-Femiano. X-rays from hot plasma in clusters of galaxies. A&A, 49:137–144, May 1976.

[16] A. Cavaliere and R. Fusco-Femiano. The Distribution of Hot Gas in Clusters of Galaxies. A&A, 70:677, November 1978.

[17] M. Birkinshaw. Measurement of the Sunyaev-Zel'dovich Effect. In A. Blanchard, L. Celnikier, M. Lachieze- Rey, and J. Tran Thanh Van, editors, *Physical Cosmology*, page 177, 1991.

[18] M. Birkinshaw. The Sunyaev-Zel'dovich effect. *Phys. Rep*, 310:97–195, March 1999. doi: 10.1016/S0370- 1573(98)00080-5.